Electrical Conductivity Transitions and Self-Assembly in Comb-Shaped Complexes of Polyaniline Based on Crystallization and Melting of the Supramolecular Side Chains

Marja Vilkman,[†,‡] Harri Kosonen,*[,†,‡] Antti Nykänen,[†] Janne Ruokolainen,[†] Mika Torkkeli,[§] Ritva Serimaa,[§] and Olli Ikkala*[,†]

Department of Engineering Physics and Mathematics, and Center for New Materials, Helsinki University of Technology, P.O. Box 2200, FI-02015 HUT, Espoo, Finland; VTT Information Technology, Microelectronics, Technical Research Center of Finland, P.O. Box 1208, FI-02044 VTT, Finland; and Department of Physical Sciences, University of Helsinki, P.O. Box 64, FI-00014 Helsinki, Finland

Received February 8, 2005; Revised Manuscript Received June 24, 2005

ABSTRACT: We report self-assembly and electronic conductivity transitions in polyaniline (PANI) where the iminic nitrogens are protonated by sulfonic acid-terminated low molecular weight poly(ethylene oxide) $CH_3-(O-C_2H_4-)_{46}-CH_2-SO_3H$ (PEOSA), i.e., which contains 46 ethylene oxide repeat units. The complex $PANI(PEOSA)_{0.5}$ self-assembles due to the comb-shaped architecture consisting of the PANI backbone and the supramolecular PEO side chains, as characterized using small- and wide-angle X-ray scattering (SAXS and WAXS) and transmission electron microscopy (TEM). PEO in the complex $PANI(PEOSA)_{0.5}$ is crystalline near room temperature; TEM and SAXS indicate lamellar self-assembly with a long period of ca. 150 Å, and the conductivity is of the order 10^{-4} S/cm. A collapse of the self-assembly periodicity to 115 Å is observed at ca. 55 °C during a slow heating at 1 °C/min, and the conductivity drops stepwise to ca. half of the value as the PEO chains melt. Even if the observed conductivity transition is still relatively small, it is reproducible and reversible upon heating and cooling, with some hysteresis. We expect that the concept can be developed to open new possibilities for responsive conjugated polymers.

Introduction

Polymeric materials that respond to external conditions and stimuli have been pursued for different functions, such as for sensors, smart coatings, selective membranes, actuators, and controlled drug release. Typically, polymer conformations and swelling of networks in aqueous solutions are controlled by temperature, pH, light, or solvent quality, which has led to e.g. responsive hydrogels, tunable surfaces containing polymer brushes, and actuators.[1−4] More recently, also solvent-free systems have been pursued. In this respect self-assembly[5−11] has proven to be useful, utilizing competing interactions to form ordered nanoscale structures. Phase transitions of the self-assembled structures have been used to achieve temperature-induced switching of protonic conductivity[12] and optical band gap.[13] Temperature-induced large conductivity switching has been observed in columnar liquid crystals of oligomeric aniline tetramer/surfactant complexes due to the order−disorder transition.[14]

On the other hand, ionically conducting solid polymeric electrolytes have been investigated for energy storage where different chain architectures of PEO with added lithium salts have been widely studied.[15−18] Upon heating conductivity typically increases stepwise by several orders of magnitude when the PEO medium melts, thus leading to an enhanced mobility of the ions. Therefore, such ionically conducting solid polymer electrolyte salts show thermoresponsive conductivity with reduced conductivity at low temperatures.

In its emeraldine base form, PANI is an intractable semiconducting polymer consisting of phenylene diamine and quinoid diimine moieties.[19,20] It is made electronically conducting by protonating the iminic nitrogens using a strong acid, which leads to a concurrent internal redox process.[21,22] Functionalized surface active and spacerlike protonating acids have been introduced.[23,24] They render enhanced solubility and fusibility and have thus paved the way for commercialization. More recently, the conductivity and the self-assembled structures of PANI salts have been tailored using different protonating acids and complexes.[20,25−27]

In this work our aim was to achieve thermally switching PANI salts using acid-terminated chainlike molecules whose conformations change as a function of temperature from extended or helical conformations to random coils due to melting. Sulfonic acid-terminated poly(ethylene oxide) (PEOSA) was chosen as a dopant because PEO is crystalline with a helical 7/2 conformation at room temperature and melts at ca. 55 °C. We used PEOSA side chains with 46 repeat units. The molecular formula of the nominally fully protonated complex between PANI and PEOSA, $PANI(PEOSA)_{0.5}$, is shown in Figure 1. The self-assembled structures are studied using TEM, SAXS, and WAXS, and the conductivity using the four-wire method.

Experimental Section

Materials. The emeraldine base form of polyaniline (PANI) was provided by Panipol Ltd. (Finland) and was used without further purification. The molecular $CH_3-(O-C_2H_4-)_{46}-CH_2-SO_3H$, i.e., PEOSA, was synthesized as described elsewhere.[28,29] PEOSA was dried at 30 °C for 1 day after the ion exchange in water.

Sample Preparation. PANI and PEOSA were dissolved in formic acid (Riedel-de Haën, purity at least 98%) separately.

[†] Helsinki University of Technology.
[‡] Technical Research Center of Finland.
[§] University of Helsinki.
* Corresponding authors. E-mail: olli.ikkala@hut.fi, hkosonen@focus.hut.fi.

10.1021/ma0502856 CCC: $30.25
Published on Web 08/04/2005

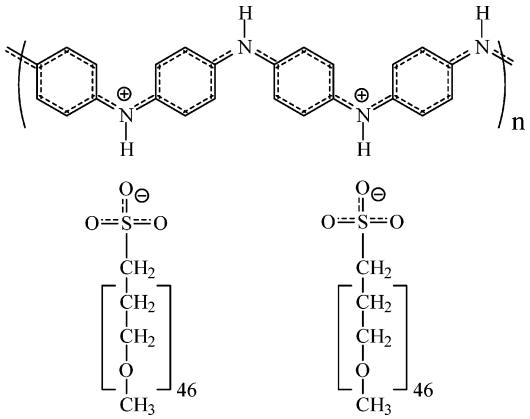

Figure 1. Molecular formula of PANI(PEOSA)$_{0.5}$ complex where all of the iminic nitrogens of PANI have nominally been protonated.

No particles were observed in solutions at the resolution of the optical microscope. PANI solution was filtered through a 0.6 μm filter. The solutions were combined to achieve PANI(PEOSA)$_x$, and the mixtures were stirred for 1 day at room temperature. Here x describes the nominal ratio of the sulfonic acid groups vs the PANI PhN repeat unit, and the following samples were prepared: $x = 0$, 0.2, 0.3, 0.4, 0.5, 0.75, and 1.0. The latter two showed evidence of macroscopic phase separation and $x = 0.5$ showed the most feasible conductivity properties. Therefore, the focus here is in PANI(PEOSA)$_{0.5}$. Formic acid was slowly evaporated at room temperature and thereafter the samples were vacuum-dried at 30 °C for 3 days. After drying, the temperature was increased to 60 °C for a few minutes, and the samples were left to cool to room temperature.

Transmission Electron Microscopy (TEM). Because of the water solubility of the PEO chains, specific techniques had to be applied. A sample of PANI(PEOSA)$_{0.5}$ was compressed between two plastic plates, and thin sections (50−100 nm) were cut from the sample using a Leica Ultracut UCT ultramicrotome and a diamond knife at −100 °C. Staining with osmium tetroxide was performed for the microtomed sections. Bright field TEM was performed using a Tecnai 12 transmission electron microscope with tungsten filament operating at an accelerating voltage of 120 kV.

Small- and Wide-Angle X-ray Scattering (SAXS and WAXS). X-ray scattering was used to study the self-assembly. Experiments were performed with a sealed X-ray tube. The Cu Kα radiation ($\lambda = 1.54$ Å) was monochromatized with a totally reflecting mirror (Huber small-angle chamber 701) and Ni filter. Distances from sample to detector were 119.5 cm (SAXS) or 8 cm (WAXS). The scattering intensities were measured using an area detector (Bruker AXS). Samples were heated from 5 to 90 °C and cooled back to 5 °C, and measurements were performed at every 5 °C, having a hold time of 1 min before each measurement.

Conductivity Measurements. The electronic conductivities were measured as a function of temperature in the temperature range 0−80 °C with a rate of 1 °C/min using the conventional four-wire technique and Keithley 2400 SourceMeter controlled with TestPoint program. Films of PANI(PEOSA)$_x$ were evaporated from a 1% formic acid solution on a cup-shaped glass plate, which had four gold electrodes evaporated on top of it. The samples were dried in a vacuum at 30 °C for 24 h and heated to 60 °C for a few minutes and cooled slowly before the measurements. The Ohmic behavior was checked by measuring the IV curves at each temperature and the voltage as a function of time with the constant current for over 1 h.

UV−Vis−NIR Spectroscopy. UV−vis−NIR spectra were measured using a Lambda 900 spectrophotometer (Perkin-Elmer) as a function of temperature from 320 to 2500 nm. PANI, PEOSA, and PANI(PEOSA)$_x$ samples were spin-cast from formic acid at 2000 rpm on quartz substrates using

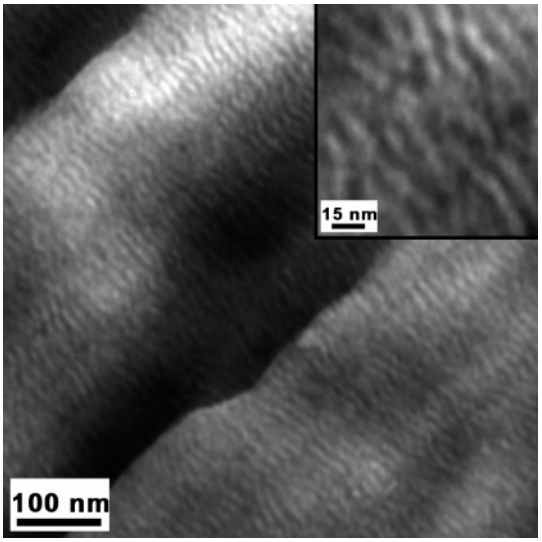

Figure 2. TEM micrograph of PANI(PEOSA)$_{0.5}$ showing a lamellar structure at room temperature.

solutions of concentration of 1%. The samples were dried in a vacuum at 30 °C for 1 day and after drying they were heated to 60 °C for a few minutes and slowly cooled to room temperature. Measurements were performed at temperatures from room temperature to 70 °C at every 5 °C.

FTIR Spectroscopy. All infrared spectra were obtained using a Nicolet Magna 750 FTIR spectrometer at temperatures ranging from 35 to 85 °C. At least 64 scans were averaged at a resolution of 2 cm^{-1}. The samples were ground with potassium bromide crystals and pressed onto pellets. The samples were dried in a vacuum oven at 30 °C for 24 h and heated to 60 °C for a few minutes before measurements.

Differential Scanning Calorimetry (DSC). DSC was performed with a Mettler Toledo Star DSC 821. The temperature was swept between 0 and 80 °C twice using the sweep rate 10 °C/min. The melting and crystallization temperatures were determined from the second temperature cycle.

Results and Discussion

It is well-known that the emeraldine base form of PANI and sulfonic acids form electronically conducting salt complexes (see the reviews[19,20]). In the case of PANI(PEOSA)$_{0.5}$, the complexation between PEOSA and PANI manifests as the formation of the characteristic polaron peaks near 400 and 800 nm in the UV−vis absorption spectrum (see later Figure 8), in the observed structures using X-ray scattering (Figure 3) and TEM (Figure 2), and the formation of plasticized material which is homogeneous in optical microscopy.

It is also known that self-assembled structures are formed if sufficiently long nonpolar alkyl side chains are used in the PANI salt complexes.[20,24,26,27,30] As in PANI(PEOSA)$_{0.5}$ both the PEO side chains and the protonated PANI backbone are polar, and in addition, PEO contains potentially hydrogen bond accepting ethers whereas PANI contains hydrogen bond donating amines; it is nontrivial whether their repulsion suffices for self-assembly (see also a closely related discussion in ref 31). The TEM micrograph of PANI(PEOSA)$_{0.5}$ (see Figure 2) confirms that self-assembly is achieved at room temperature and that the structure is lamellar. TEM suggests that the periodicity is in the range of 140 Å. As will be discussed subsequently, the proposed structure consists of alternating PANI and crystalline PEO lamellae.

The structure of PANI(PEOSA)$_{0.5}$ was studied as a function of temperature using WAXS and SAXS (see

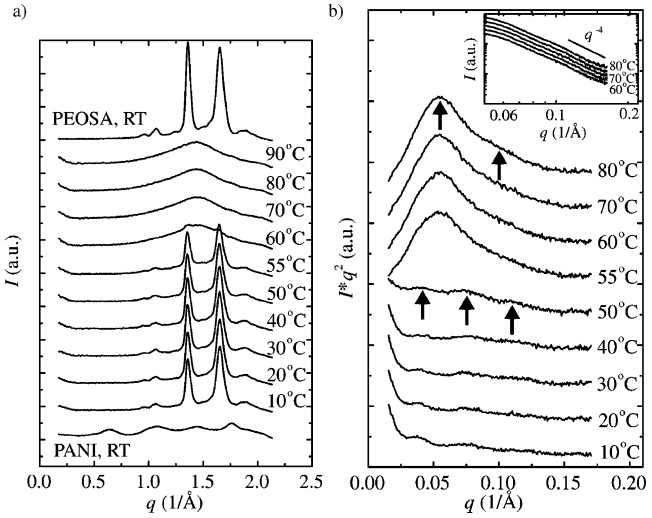

Figure 3. (a) WAXS and (b) SAXS curves for PANI(PEOSA)$_{0.5}$ during heating. They are reversible in heating and cooling with a little hysteresis. WAXS data of PANI and PEOSA at room temperature are shown for reference. The magnitude of the scattering vector is given by $q = (4\pi/\lambda) \sin \theta$, where 2θ is the scattering angle and $\lambda = 1.54$ Å.

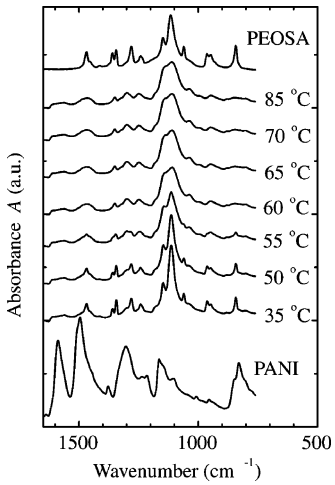

Figure 4. FTIR data for PANI, PEOSA, and the complex of PANI(PEOSA)$_{0.5}$ as a function of temperature. During heating the positions of many of the peaks shift at a temperature of ca. 55 °C, indicating the melting of PEO crystals. PANI and PEOSA at room temperature are shown for reference.

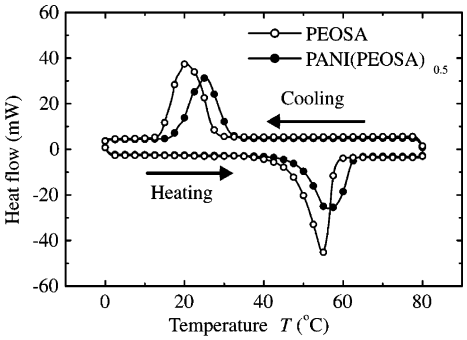

Figure 5. DSC results for PANI(PEOSA)$_{0.5}$ and pure PEOSA.

Figure 3). PANI cast from formic acid shows WAXS reflections (see Figure 3a) that are almost identical to those reported for PANI protonated using HCl (the crystalline structure ES-I[32]), as the protonated crystalline structure is "frozen" before the formic acid has been totally removed. Such reflections are not observed in PANI(PEOSA)$_{0.5}$, but instead, reflections characteristic of PEO are observed, confirming that the side chains consisting 46 ethylene oxide repeat units undergo side chain crystallization which has a similar scattering pattern as bulk PEO. WAXS further confirms that the supramolecular PEO side chains of PANI(PEOSA)$_{0.5}$ melt at 55−60 °C. The phenomenon was reversible upon cooling, showing a slight hysteresis. SAXS data in Figure 3b show only weak reflections near room temperature, but interestingly three orders of reflections can be observed at $q_1^* = 0.040$ Å^{-1}, $2q_1^*$, and $3q_1^*$. This suggests a lamellar structure with a long period of ca. 150 Å at $T <$ ca. 50 °C. We expect that the weak intensity results from a small electron density contrast between the layers: fully crystalline PANI has an estimated electron density $\rho_e = 0.44$ Å^{-3} whereas crystalline PEO has $\rho_e = 0.39$ Å^{-3}. Only hand-waving arguments can here be given for the corresponding values of PANI(PEOSA)$_{0.5}$: the PEO side chains in PANI(PEOSA)$_{0.5}$ are relatively highly crystalline, and therefore, the electron density is expected to be rather high, approaching that of the bulk crystalline PEO. By contrast, the crystallinity within the PANI layers was effectively suppressed, leading to a large reduction of electron density. Therefore, the electron density contrast between the PANI and PEO layers is expected to be small, leading to weak reflections. When PEO chains melt above ca. 55 °C, the electron density of the PEO layers is considerably reduced. The electron density difference between melt PEO and PANI is therefore increased, and increased scattering intensity is expected. Indeed, Figure 3b shows that upon melting the scattering intensity increases, and the maximum is observed at $q_2^* = 0.055$ Å^{-1}. The reflection is broad, and a very weak higher order reflection is barely observable at $2q_2^*$ which suggests that the structure is lamellar with the periodicity of 115 Å. Additional support that self-assembly is indeed observed instead of correlation hole effects without structure is shown in the inset of Figure 3b, which indicates that Porod's law is obeyed, i.e., $I \propto q^{-4}$. It suggests that there are interfaces within the system and that at $T >$ 60 °C the reflections, even if relatively broad, are due to self-assembled structures and not due to correlation hole effects.

Crystallization and melting of the supramolecular PEO side chains of PANI(PEOSA)$_{0.5}$ were also studied using FTIR spectroscopy (Figure 4). The absorption peaks correspond to the results previously presented for crystalline PEO (2945, 2885, 1360, 1343, 1280, 1242, 1149, 1108, 1060, 962, and 946 cm^{-1}) and the amorphous PEO (2948, 2866, 1350, 1325, 1297, 1249, 1108, and 949 cm^{-1}).[33]

Differential scanning calorimetry (DSC) measurements were performed in the temperature range of 0−80 °C for PANI, PEOSA, and PANI(PEOSA)$_x$ with different x using the sweep rate of 10 °C/min (see Figure 5 for PEOSA and $x = 0.5$). PANI did not show transitions at this temperature range, whereas PEOSA and PANI(PEOSA)$_x$ underwent melting at ca. 55−57 °C during heating and crystallization at ca. 20−25 °C during cooling. These transition temperatures are in line with those observed with SAXS, WAXS, and conductivity measurements. The extent of hysteresis depends on the heating and cooling rate and can obviously be reduced if slower temperature sweeps were used.

Samples were analyzed also using polarized optical microscopy and PANI(PEOSA)$_{0.5}$ was birefringent for $T <$ ca. 55 °C and optically isotropic for $T >$ ca. 55 °C.

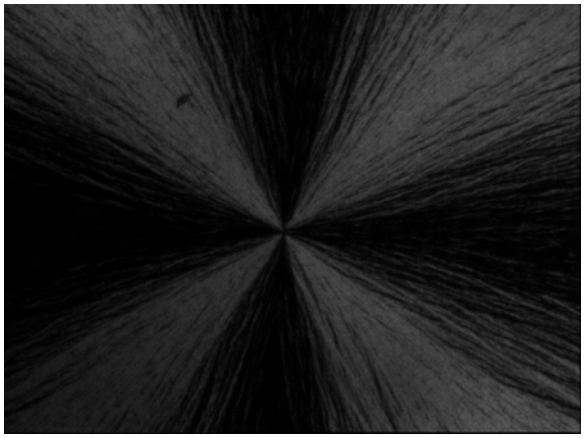

Figure 6. Optical microscope picture of PANI(PEOSA)$_{0.5}$ using crossed polarizers at room temperature showing a birefringent spherulitic-like structure. For comparison at 60 °C the sample is optically isotropic.

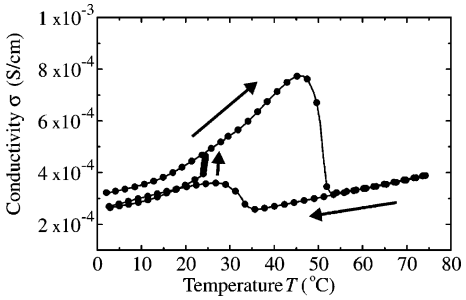

Figure 7. Electronic conductivity of PANI(PEOSA)$_{0.5}$ as a function of temperature using a sweep rate of 1 °C/min, showing a conductivity transition when the supramolecular PEO side chains melt or crystallize. The directions of the heating and cooling are marked with arrows. Hysteresis between the heating and cooling is observed, indicating kinetic effects. After cooling to room temperature, conductivity returns to its original value within a few hours. All conductivity values correspond to Ohmic behavior, as measured using four-wire method.

The optical microscope picture of PANI(PEOSA)$_{0.5}$ at room temperature is shown in Figure 6.

The conductivity of PANI(PEOSA)$_{0.5}$ is depicted in Figure 7 as a function of heating and cooling using the sweep rate 1 °C/min. At first, the conductivity increases smoothly with increasing temperature obviously due to thermal activation, but at ca. 53 °C it decreases stepwise. Above this transition, the conductivity continues to increase again. Cooling leads to a corresponding conductivity transition, and hysteresis of ca. 20 °C between heating and cooling was observed. The crystallization is a relatively slow process and the sweep rate 1 °C/min does not allow sufficient time for the PEO side chains to crystallize completely between the repeated cycles. Therefore, the original conductivity was not fully recovered during continued cycling at 1 °C/min. However, the conductivity retained the original value during a few hours upon standing at room temperature as the crystallization process completed. The smoothly increased; i.e., activated conductivity during heating is typical for a material containing disordered polyaniline regions with localized electrons,[34] which could be expected also in our case, as the conductivity is relatively low. Note that conductivity transitions due to side chain melting have not been reported before.

To gain further understanding on the conductivity transition, PANI(PEOSA)$_{0.5}$ was analyzed also using

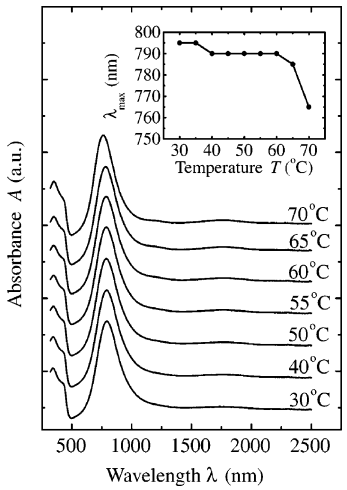

Figure 8. UV−vis−NIR curves for PANI(PEOSA)$_{0.5}$ as a function of temperature. A slight blue shift of the polaron peak at T > 60 °C is observed. The inset shows λ_{max} as a function of temperature.

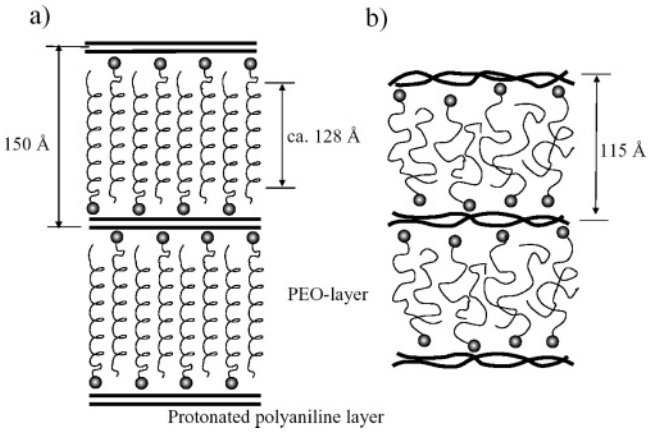

Figure 9. Schematic of the structure of PANI(PEOSA)$_{0.5}$. (a) When the PEO side chains are crystalline, the long period is ca. 150 Å and the self-assembled structure is relatively well ordered. (b) When the side chains melt, the long period is reduced to ca. 115 Å and the disorder is increased.

UV−vis−NIR as a function of temperature (see Figure 8). PEOSA did not have a significant absorbance in the measured wavelength range, and the undoped PANI had an absorption peak near 600 nm due to exciton absorption of the quinoid rings, as expected.[19] In PANI(PEOSA)$_{0.5}$ this peak was suppressed, and a new peak at ca. 800 nm was observed, demonstrating the complexation between PANI and PEOSA and providing evidence for the localized polaron bands of the salt.[35] An increased absorbance above 1000 nm due to the free carrier tail[35] was not, however, observed, which is in line with the relatively low conductivity where the electrons are not delocalized. The UV−vis−NIR spectra were studied as a function of temperature. Below the PEOSA side-chain melting temperature, the UV−vis−NIR curves were essentially similar. By contrast, above this temperature, a blue shift of 30 nm was seen. The effect is small, but still it suggests that PANI may adapt a slightly more elongated structure and improved order at low temperatures when the confining PEO side chains are crystalline. When the side chains melt, the PANI chains may have more freedom to rotate and thus the band gap increases, as implied by the blue shift.[36,37]

The schematic picture in Figure 9 shows the suggested self-assembled structure of PANI(PEOSA)$_{0.5}$

below and above the side chain melting transition. Near room temperature, i.e., when the PEO side chains are crystalline, SAXS shows a lamellar structure with a periodicity of ca. 150 Å, which roughly agrees also with the TEM observations. In the crystalline bulk state the PEO chains form 7/2 helices and pack into the crystal structure of the $P2_{1/a}$ space group.[38] The WAXS and FTIR data of this work suggest that in $PANI(PEOSA)_{0.5}$ the crystalline structure of the PEO layers is similar to that of the bulk PEO phase. Taken the packing, one therefore expects that 46 EO repeat units form a layer of thickness of ca. 128 Å. In a closely related study dealing with structures of PANI complexed with phosphoric acid-terminated PEO (where the conductivity issues were, however, not discussed), the PANI layers were estimated to have a thickness of ca. 17 Å.[31] Therefore, it is suggested that a bilayer structure is formed, as illustrated in Figure 9a, where the PANI chains within the layers would be relatively well organized due to confinement exerted by the ordered crystalline packing of the PEO side chains. Upon side-chain melting, the order in the PEO layers is suppressed, leading to coiled conformations of the PEO chains and the collapse of the periodicity. This may lead to less organized PANI layers with slightly reduced conductivity.

Finally, we point out that in the present case dealing with electronic conductivity the conductivity level drops upon the melting of PEO. This may emphasize the importance of order to promote electronic conductivity. This contrasts to the classical case of solid polymer electrolytes consisting of PEO with immobilized lithium salts, where the ionic conductivity is improved when the PEO medium melts.[15−18]

Conclusions

PANI protonated with low molecular weight poly(ethylene oxide) sulfonic acid with 46 ethylene oxide repeat units is studied. Lamellar self-assembly is obtained with alternating PANI and PEO layers. Near room temperature the periodicity is ca. 150 Å, and the PEO side chains are crystalline. The conductivity level is on the order of 10^{-4} S/cm. Upon heating above the melting transition of the PEO side chains, the conductivity drops stepwise to half of the value just below the transition. Upon cooling, the original conductivity value is regained after a hysteresis. A possible reason for the conductivity transition is suggested on the basis of reduced order and more coiled conformations of PANI when the PEO side chains are molten, as also a slight blue shift was observed in the electronic spectrum of the complex in this case.

We expect that tuning the length of the side chains allows us to control the switching ratios. Different side chains can be used to tailor the switching temperatures. Such materials could be used e.g. in sensor applications. Even though the material cannot yet compete in accuracy, speed, and stability with the conventional temperature sensors, it could find use for example in large-scale products of the packaging industry as an economic and flexible temperature sensor.

Acknowledgment. We thank Hannele Eerikäinen for the synthesis of the sulfonic acid-terminated poly(ethylene oxide) and Heikki Tenhu, Franciska Sundholm, Miia Hiltunen, and Antti Lamminpää for discussions. We are grateful for PANIPOL Ltd. (Finland) for providing polyaniline. We acknowledge grants from National Technology Agency of Finland (in part Grants PAFU and POTRA) and Center of Excellence of Academy of Finland ("Bio- and Nanopolymers Research Group", 77317).

References and Notes

(1) Okano, T. *Biorelated Polymers and Gels*; Academic Press: Boston, 1998.
(2) Khan, I. M.; Harrison, J. S. *Field Responsive Polymers*: *Electroresponsive, Photoresponsive, and Responsive Polymers in Chemistry and Biology*; American Chemical Society: Washington, DC, 1999.
(3) Urry, D. W. *Trends. Biotechnol.* **1999**, *17*, 249.
(4) Wallace, G. G.; Spinks, G. M.; Teasdale, P. R. *Conductive Electroactive Polymers; Intelligent Materials Systems*; Technomic Publishing: Lancaster, 1997.
(5) Whitesides, G. M.; Grzybowski, B. *Science* **2002**, *295*, 2418.
(6) Muthukumar, M.; Ober, C. K.; Thomas, E. L. *Science* **1997**, *277*, 1225.
(7) Hamley, I. W. *Angew. Chem., Int. Ed.* **2003**, *42*, 1692.
(8) Antonietti, M.; Burger, C.; Effing, J. *Adv. Mater.* **1995**, *7*, 751.
(9) Ruokolainen, J.; ten Brinke, G.; Ikkala, O. T. *Adv. Mater.* **1999**, *11*, 777.
(10) Ikkala, O.; ten Brinke, G. *Science* **2002**, *295*, 2407.
(11) Antonietti, M. *Nat. Mater.* **2003**, *2*, 9.
(12) Ruokolainen, J.; Mäkinen, R.; Torkkeli, M.; Mäkelä, T.; Serimaa, R.; ten Brinke, G.; Ikkala, O. *Science* **1998**, *280*, 557.
(13) Valkama, S.; Kosonen, H.; Ruokolainen, J.; Torkkeli, M.; Serimaa, R.; ten Brinke, G.; Ikkala, O. *Nat. Mater.* **2004**, *3*, 872.
(14) Wei, Z.-X.; Laitinen, T.; Smarsly, B.; Ikkala, O.; Faul, C. F. J. *Angew. Chem., Int. Ed.* **2005**, *44*, 751.
(15) Gray, F. M. *Polymer Electrolytes*; The Royal Society of Chemistry: Cambridge, 1997.
(16) Angell, C. A.; Xu, K.; Zhang, S.-S.; Videa, M. *Solid State Ionics* **1996**, *86−88*, 17.
(17) Richardson, T. H. *Functional Organic and Polymeric Materials*; *Molecular Functionality-Macroscopic Reality*; Wiley & Sons, Ltd.: Chichester, 2000.
(18) Wright, P. V. *MRS Bull.* **2002**, *27*, 597.
(19) Skotheim, T. A.; Elsenbaumer, R. L.; Reynolds, J. R. *Handbook of Conducting Polymers*, 2nd ed.; Marcel Dekker: New York, 1998.
(20) Pron, A.; Rannou, P. *Prog. Polym. Sci.* **2002**, *27*, 135.
(21) Doriomedoff, M.; Hautiere-Cristofini, F.; Surville, R. D.; Jozefowicz, M.; Yu, L.-T.; Buvet, R. *J. Chim. Phys. Physicochim. Biol.* **1971**, *68*, 1055.
(22) Chiang, J.-C.; MacDiarmid, A. G. *Synth. Met.* **1986**, *13*, 193.
(23) Cao, Y.; Smith, P.; Heeger, A. J. *Synth. Met.* **1992**, *48*, 91.
(24) Zheng, W.-Y.; Wang, R.-H.; Levon, K.; Rong, Z. Y.; Taka, T.; Pan, W. *Makromol. Chem. Phys.* **1995**, *196*, 2443.
(25) Pomfret, S. J.; Adams, P. N.; Comfort, N. P.; Monkman, A. P. *Adv. Mater.* **1998**, *10*, 1351.
(26) Kosonen, H.; Ruokolainen, J.; Knaapila, M.; Torkkeli, M.; Jokela, K.; Serimaa, R.; ten Brinke, G.; Bras, W.; Monkman, A. P.; Ikkala, O. *Macromolecules* **2000**, *33*, 8671.
(27) Dufour, B.; Rannou, P.; Djurado, D.; Janeczek, H.; Zagorska, M.; de Geyer, A.; Travers, J.-P.; Pron, A. *Chem. Mater.* **2003**, *15*, 1587.
(28) Hamaide, T.; Le Deore, C. *Polymer* **1993**, *34*, 1038.
(29) Herranen, J.; Kinnunen, J.; Mattsson, B.; Rinne, H.; Sundholm, F.; Torell, L. *Solid State Ionics* **1995**, *80*, 201.
(30) Tiitu, M.; Volk, N.; Torkkeli, M.; Serimaa, R.; ten Brinke, G.; Ikkala, O. *Macromolecules* **2004**, *37*, 7364.
(31) Nandan, B.; Chen, H.-L.; Liao, C.-S.; Chen, S.-A. *Macromolecules* **2004**, *37*, 9561.
(32) Pouget, J. P.; Józefowicz, M. E.; Epstein, A. J.; Tang, X.; MacDiarmid, A. G. *Macromolecules* **1991**, *24*, 779.
(33) Su, Y.; Wang, J.; Liu, H. *Langmuir* **2002**, *18*, 5370.
(34) Epstein, A. J.; MacDiarmid, A. G. *Synth. Met.* **1995**, *69*, 179.
(35) Xia, Y.; Wiesinger, J. M.; MacDiarmid, A. G.; Epstein, A. J. *Chem. Mater.* **1995**, *7*, 443.
(36) McCullough, R. D.; Lowe, R. D.; Jayaraman, M.; Anderson, D. L. *J. Org. Chem.* **1993**, *58*, 904.
(37) Ho, K.-S. *Synth. Met.* **2002**, *126*, 151.
(38) Takahashi, Y.; Tadokoro, H. *Macromolecules* **1973**, *6*, 672.

MA0502856